

# Fine structure of the exciton absorption in semiconductor superlattices in crossed electric and magnetic fields

B. S. Monozon

*Physics Department, Marine Technical University,  
3 Lotsmanskaya Str., 190121 St.-Petersburg, Russia*

V. G. Bezchastnov\*

*Institute of Physical Chemistry, University of Heidelberg,  
INF 229, 69120 Heidelberg, Germany*

P. Schmelcher

*Zentrum für Optische Quantentechnologien, Universität Hamburg,  
Luruper Chaussee 149, 22761 Hamburg, Germany and  
The Hamburg Centre for Ultrafast Imaging, Universität Hamburg,  
Luruper Chaussee 149, 22761 Hamburg, Germany*

(Dated: October 26, 2018)

## Abstract

The exciton absorption coefficient is determined analytically for a semiconductor superlattice in crossed electric and magnetic fields, for the magnetic field being parallel and the electric field being perpendicular to the superlattice axis. Our investigation applies to the case where the magnetic length, while being much smaller than the exciton Bohr radius, considerably exceeds the superlattice period. The optical absorption in superlattices displays a spectral fine structure related to the sequences of exciton states bound whose energies are adjacent to the Landau energies of the charge carriers in the magnetic field. We study effects of external fields and of the centre-of-mass exciton motion on the fine structure peak positions and oscillator strengths. In particular, we find that the inversion of the orientation of the external fields and of the in-plane total exciton momentum notably affects the absorption spectrum. Conditions for the experimental observation of the exciton absorption are discussed.

---

\* On leave from: Ioffe Physical-Technical Institute, 194021 St.-Petersburg, Russia; Present address: Max Planck Institute for Medical Research, Jahnstrasse 29, 69120 Heidelberg

## I. INTRODUCTION

Semiconductor Superlattices (SL) are since a few decades in the focus of intense theoretical and experimental research. Starting from the studies by Esaki and Tsu [1], a vivid interest exists in the electronic, transport and optical properties of SLs. The presence of external electric  $\vec{F}$  and magnetic  $\vec{B}$  fields is known to strongly influence these properties, in particular due to the electric Wannier-Stark (WS) [2] and the magnetic Landau [3] quantizations of the electronic motion.

Different field orientations have been considered for the situations where SL are exposed to either an electric or a magnetic field, or to both fields. For example, the quantization effects in the optical response of SL were investigated for  $\vec{F} \parallel \vec{e}_z$  in Refs. [4–7] and for  $\vec{B} \parallel \vec{e}_z$  in Refs. [8, 9], where the unit vector  $\vec{e}_z$  determines the direction of the SL axis. Combined effects of both fields on the interband optical transitions were studied by Pacheco *et.al.* [10] for  $\vec{F} \parallel \vec{B} \parallel \vec{e}_z$ . Suris *et.al.* calculated the energy spectrum [11], optical absorption coefficient [12] and magnetoresistivity [13] for crossed fields - longitudinal electric,  $\vec{F} \parallel \vec{e}_z$ , and in-plane magnetic field  $\vec{B} \perp \vec{e}_z$ . For the same field geometry, Zuleta and Reyes-Gomes [14] have recently investigated the interband optical absorption spectra of a GaAs/GaAlAs variably spaced SL.

According to the experimental measurements [15, 16], the electronic and optical properties of quasi-2D semiconductor structures are notably influenced by the excitons - the electron-hole pairs bound by the Coulomb attraction. For SLs exposed to parallel ( $\vec{B} \parallel \vec{F} \parallel \vec{e}_z$ ) and crossed ( $\vec{F} \parallel \vec{e}_z$ ,  $\vec{B} \perp \vec{e}_z$ ) fields, exciton effects were considered in Ref. [17] and Ref. [18], respectively. A variety of studies on SL excitons in external fields are described in the reviews and monographs [19–21].

Despite the fact that basic properties of SL excitons are comprehensively studied, some qualitatively novel results have been reported recently. Suris [22] has revealed and analytically investigated an interplay between the center-of-mass and relative motions of excitons in a semiconductor SL. This effect results from the deviation of the dispersion for the exciton electron-hole pair from a quadratic law and leads to a fine structure of the exciton Rybderg states. A similar structure was studied earlier by Kohn and Luttinger [23] for the Ge and Si bulk crystals with extremely anisotropic isoenergy band surfaces.

The works [22, 23] do not address situations where external fields are applied to SL.

For a longitudinal electric field,  $\vec{F} \parallel \vec{e}_z$ , the fine structure of the exciton absorption was studied in Ref. [24]. The binding energies  $E_n^{(b)}$  and the oscillator strengths  $f_n$  of the fine structure states  $n = 0, 1, 2, \dots$  were shown to be of the order of  $4\text{Ry}/(2n+1)^2$  and  $1/(a_0^2\bar{z})$ , respectively, where  $\text{Ry} \sim a_0^{-2}$  is the exciton Rydberg constant,  $a_0$  is the exciton Bohr radius, and  $\bar{z} \sim d^{2/3}(\Delta_e + \Delta_h)^{1/3}$  is the longitudinal size of the exciton. This size is determined by the SL period  $d$  and the miniband widths  $\Delta_e$  for the electrons and  $\Delta_h$  for the holes, with the widths being dependent on the longitudinal exciton momentum in the electric field applied.

The studies [22, 24] employ the adiabatic,  $2\bar{z} \ll a_0$ , and the continual,  $d \ll \bar{z}$ , approximations which facilitate the analytical calculations. Justifying both approximations requires the condition  $2d \ll a_0$  which, as already pointed out in Ref. [22], might not be well satisfied in typical SLs. For example, for the GaAs/AlGaAs SL with a period of 2 nm, the Bohr radius  $a_0 = 11.4$  nm does not significantly exceed the value  $2d = 4$  nm to provide the adiabatic and continual approximations. On the other hand, with increasing  $a_0$  the exciton binding energies and oscillator strengths decrease being both proportional to  $a_0^{-2}$ . This makes the crystals with larger values for the exciton Bohr radius less suitable for an experimental probing of the fine structure. However, the presence of an external magnetic field can increase both the binding energies and the oscillator strengths making thereby the fine spectral structure more pronounced as compared to the case without the field. Theoretical calculations of the fine structure in the presence of the external fields are therefore of fundamental interest and relevant for supporting the experimental studies.

In the present paper we consider a SL of a short period  $d \ll a_0$  subject to crossed external electric  $\vec{F}$  and magnetic  $\vec{B}$  fields. We focus on an analytical investigation and analysis of the exciton bound states and optical absorption. The external magnetic field is assumed to be stronger than the exciton internal field providing the magnetic length  $a_B = \sqrt{\hbar/(eB)}$  to be much smaller than the exciton Bohr radius  $a_0$ . Thus, for the magnetic field directed along the SL axis, we study a regime where the in-plane exciton size  $\sim a_B$  becomes much smaller than this size  $\sim a_0$  in the absence of the field and leads to a significant increase of the fine structure binding energies and oscillator strengths. We show that the presence on an in-plane electric field results in additional exciton peaks in the magneto-absorption spectrum. The impact of the combined magnetic and electric fields on the exciton bound states is studied in detail. In particular, we investigate a coupling between the longitudinal and in-plane collective motions of the exciton, the internal motion, and external fields. To

deliver close-form analytical results we consider a simple band model of SL and employ tight-binding, adiabatic ( $\bar{z} \ll a_B \ll a_0$ ) and continual ( $d \ll \bar{z}$ ) approximations for the exciton states and corresponding optical absorption coefficients.

The paper is organized as follows. The theoretical framework to describe the exciton states for the SL in the presence of crossed electric and magnetic fields is given in Section 2. The energies and wave functions of the bound states are presented in explicit form in Section 3. In Section 4 we determine the absorption coefficient and analyze its dependencies on the SL parameters, on the external field strengths, and on the total exciton momentum. The applicability of the obtained results is discussed and expected experimental values are estimated. Our concluding remarks are given in Section 5.

## II. GENERAL APPROACH

The Hamiltonian describing a Wannier-Mott exciton has the form

$$H_{\text{ex}} = \sum_j H_j + U, \quad (1)$$

where  $j$  designates an electron ( $j = e$ ) and a hole ( $j = h$ ) with the effective masses  $m_j$  and the charges  $e_j$  ( $e_e = -e_h = -e$ ) linked to each other by an attractive Coulomb potential

$$U = -\frac{1}{4\pi\epsilon_0\epsilon} \cdot \frac{e^2}{r}, \quad (2)$$

with  $\epsilon$  being a semiconductor dielectric constant, and  $r = |\vec{r}_e - \vec{r}_h|$  being the distance between the electron and hole located at  $\vec{r}_e$  and  $\vec{r}_h$ , respectively. The Hamiltonian (1) and the effective mass approximation apply to semiconductors with parabolic, non-degenerate, and spherically symmetric energy bands separated by a wide energy gap  $E_g$ .

In a semiconductor SL exposed to uniform external fields the Hamiltonians  $H_j$  are

$$H_j = -\frac{\hbar^2}{2m_j} \frac{\partial^2}{\partial z_j^2} + V_j + H_{\perp j} + e_j \vec{F} \vec{\rho}_j, \quad (3)$$

where  $z_j$  and  $\vec{\rho}_j$  are the longitudinal and transverse components of  $\vec{r}_j = (\vec{\rho}_j, z)$  with respect to the SL axis,  $V_j = V_j(z_j)$  are the potentials of the SL layers, and

$$H_{\perp j} = \frac{1}{2m_j} \left( -i\hbar \frac{\partial}{\partial \vec{\rho}_j} + \frac{e_j}{2} \vec{B} \times \vec{\rho}_j \right)^2 \quad (4)$$

are the kinetic energies of the motions of the electron and the hole transversely to the magnetic field. The above equation explicitly accounts for the field orientations  $\vec{F} \perp \vec{e}_z$  and  $\vec{B} \parallel \vec{e}_z$ , and the symmetrical gauge of the magnetic vector-potential is employed in  $H_{\perp j}$ .

We follow an approach described in details in Refs. [22, 24] and present below a brief outline of intermediate calculations. The SL potentials are periodic functions  $V_j(z_j) = V_j(z_j + n_j d)$  with the period  $d$  formed by a large number  $n_j = 0, 1, \dots, N_0$  of quantum wells separated by weakly penetrable barriers. We assume the size-quantized energies  $b_j \sim \hbar^2/(m_j d^2)$  to significantly exceed the miniband widths  $\Delta_j$  and apply a nearest-neighbor tight-binding approximation for the inter-well tunneling.

Expanding an eigenfunction of the Hamiltonian (1) in a set of orthonormalized Wannier functions  $w_j(z_j - n_j d)$ ,

$$\Psi(\vec{r}_e, \vec{r}_h) = \sum_{n_e, n_h} \Phi(n_e, \vec{\rho}_e; n_h, \vec{\rho}_h) w_e(z_e - dn_e) w_h(z_h - dn_h), \quad (5)$$

and exploiting conservation of the exciton transverse  $\vec{K}$  and longitudinal  $Q$  momenta, one can obtain

$$\Phi(n_e, \vec{\rho}_e; n_h, \vec{\rho}_h) = e^{i\alpha(\vec{R}_{\perp}, \vec{\rho})} g(n, \vec{\rho}), \quad (6)$$

where  $\vec{R}_{\perp} = (m_e \vec{\rho}_e + m_h \vec{\rho}_h)/M$  and  $\vec{\rho} = \vec{\rho}_e - \vec{\rho}_h$  are the center-of-mass and relative transverse coordinates, respectively,  $M = m_e + m_h$  is the exciton mass,  $n = n_e - n_h$ ,

$$\begin{aligned} \alpha(\vec{R}_{\perp}, \vec{\rho}) &= \left( \vec{K} + \frac{e}{2\hbar} \vec{B} \times \vec{\rho} \right) \vec{R}_{\perp} + \frac{\delta}{2} \vec{K}' \vec{\rho} + \frac{Qd}{2} (n_e + n_h) - \gamma dn, \\ \delta &= \frac{m_h - m_e}{M}, \quad \gamma = \frac{1}{d} \tan^{-1} \left[ \frac{\Delta_e - \Delta_h}{\Delta_e + \Delta_h} \tan \left( \frac{Qd}{2} \right) \right], \\ \vec{K}' &= \vec{K} + \frac{M}{\hbar B^2} \vec{B} \times \vec{F}. \end{aligned} \quad (7)$$

We consider a regime  $a_B \ll a_0$  where the external magnetic field dominantly determines the internal exciton motion in the coordinate  $\vec{\rho}$  and the function  $g(n, \vec{\rho})$  has the form

$$g(n, \vec{\rho}) = \Lambda_{Nm}(\vec{\rho} - \vec{\rho}_0) \psi(n), \quad (8)$$

where  $\Lambda_{Nm}(\vec{\rho} - \vec{\rho}_0)$  with  $N = 0, 1, 2, \dots$  and  $m = 0, \pm 1, \pm 2, \dots$  are the Landau functions describing relative motion of the charges  $\pm e$  in the magnetic field with respect to the center

$$\vec{\rho}_0 = \frac{\hbar}{eB^2} \vec{B} \times \vec{K}'. \quad (9)$$

The set  $\Lambda_{Nm}$  is orthonormalized,  $\langle \Lambda_{Nm} | \Lambda_{N'm'} \rangle = \delta_{NN'} \delta_{mm'}$ , and is given by the expressions

$$\begin{aligned}\Lambda_{Nm}(r_\perp, \varphi) &= \frac{e^{im\varphi}}{\sqrt{2\pi}} R_{Nm}(r_\perp), \\ R_{Nm}(r_\perp) &= \frac{1}{a_B} \sqrt{\frac{N!}{(N+|m|)!}} u^{\frac{|m|}{2}} e^{-\frac{u}{2}} L_N^{|m|}(u),\end{aligned}\quad (10)$$

where  $r_\perp^2 = (\rho_x - \rho_{0x})^2 + (\rho_y - \rho_{0y})^2$ ,  $\varphi = \tan^{-1}[(\rho_y - \rho_{0y})/(\rho_x - \rho_{0x})]$ ,  $u = r_\perp^2/(2a_B^2)$ , and  $L_N^{|m|}$  are the associated Laguerre polynomials.

The search for an eigenfunction of the Hamiltonian (1) in the form determined by Eqs. (5), (6) and (8) leads to the equation for the function  $\psi(n)$  and energies  $W_{Nm}$ :

$$\frac{\Delta_{eh}}{4} [2\psi(n) - \psi(n+1) - \psi(n-1)] + [\bar{U}_{Nm}(n; \rho_0) - W_{Nm}] \psi(n) = 0, \quad (11)$$

where  $\Delta_{eh}$  is a reduced electron-hole miniband given by the relation [22],

$$\Delta_{eh}^2 = (\Delta_e + \Delta_h)^2 - 2\Delta_e \Delta_h [1 - \cos(Qd)], \quad (12)$$

$\bar{U}_{Nm}(n; \rho_0)$  is the average of the electron-hole interaction potential (2) with the product of the densities  $|w_e(z_e - dn_e)|^2$ ,  $|w_h(z_h - dn_h)|^2$ , and  $|\Lambda_{N,m}(\vec{\rho} - \vec{\rho}_0)|^2$ , and  $W_{Nm}$  determines the exciton energy

$$E = \mathcal{E}_g + T(Q) + \frac{\hbar^2}{2M} (K^2 - K'^2) + \frac{\hbar e B}{2\mu} (2N + |m| + \delta \cdot m + 1) + W_{Nm}. \quad (13)$$

In Eq. (13),  $\mathcal{E}_g = E_g + b_e + b_h$  is the SL energy gap ( $b_e$  and  $b_h$  are the size-quantized energies of the electron and the hole, respectively),

$$T(Q) = \frac{1}{2} [\Delta_e + \Delta_h - \Delta_{eh}(Q)] \quad (14)$$

is the energy of the center-of-mass longitudinal motion, whereas the third and fourth terms describe the energies of Landau  $Nm$ -levels shifted due to the effects of the in-plane electric field  $\vec{F}$  and the exciton motion with the momentum  $\vec{K}$ .

For the exciton states with the longitudinal size exceeding significantly the SL period,  $\bar{z} \gg d$ , one can replace

$$nd \rightarrow z, \quad \psi(n+1) + \psi(n-1) - 2\psi(n) \rightarrow d^2 \psi''(z), \quad (15)$$

where  $z = z_e - z_h$  is the exciton relative coordinate. This establishes a continual approximation to Eq. (11):

$$\psi''(z) + \frac{2m_\parallel(Q)}{\hbar^2} [W_{Nm} - \bar{U}_{Nm}(z; \rho_0)] \psi(z) = 0, \quad (16)$$

where

$$m_{\parallel}(Q) = \frac{2\hbar^2}{d^2\Delta_{eh}(Q)} \quad (17)$$

has the meaning of a reduced “longitudinal” effective mass of the exciton determined by its longitudinal momentum  $Q$ , and

$$\bar{U}_{Nm}(z; \rho_0) = \frac{2}{\pi} \int_0^\infty \rho d\rho R_{Nm}^2(\rho) \frac{F(\pi/4, k) + F(\phi, k)}{\sqrt{(\rho + \rho_0)^2 + z^2}} \quad (18)$$

is an effective binding potential. The function  $F(\phi, k)$  is an elliptic integral of first kind [26],

$$\phi = \sin^{-1} \sqrt{\frac{(\rho + \rho_0)^2 + z^2}{2(\rho^2 + \rho_0^2 + z^2)}}, \quad k^2 = \frac{4\rho\rho_0}{(\rho + \rho_0)^2 + z^2}, \quad \rho_0 = \sqrt{\rho_{0x}^2 + \rho_{0y}^2}. \quad (19)$$

In the following we study bound solutions of Eq. (16) distinguished by a discrete quantum number  $p = 0, 1, 2, \dots$ . Having obtained the bound-state energies  $W_{Nm} = W_{Nmp}$  and the corresponding functions  $\psi_p(z)$ ,  $\langle \psi_p | \psi_{p'} \rangle = \delta_{pp'}$ , we can determine the exciton total energy  $E = E_{\vec{K}QNmp}$  according to Eq. (13) and determine the wave functions

$$\begin{aligned} \Psi_{\vec{K}QNmp}(\vec{r}_e, \vec{r}_h) &= d \sum_{n_e, n_h} w(z_e - dn_e) w(z_h - dn_h) \frac{e^{i\beta_{\vec{K}Q}(\vec{r}_e, \vec{r}_h)}}{\sqrt{SL}} \Lambda_{Nm}(\vec{\rho} - \vec{\rho}_0) \psi_p(z), \\ \beta_{\vec{K}Q}(\vec{r}_e, \vec{r}_h) &= \vec{K} \vec{R}_\perp + QZ + \frac{e}{2\hbar} (\vec{B} \times \vec{\rho}) \cdot \vec{R}_\perp + \frac{\delta}{2} \vec{K}' \cdot \vec{\rho} - \frac{1}{2} \frac{\Delta_e - \Delta_h}{\Delta_e + \Delta_h} Qz, \end{aligned} \quad (20)$$

where  $Z = (z_e + z_h)/2$  (notice that for equal electron and hole masses  $Z$  coincides with the exciton longitudinal center-of-mass coordinate). With  $L = N_0d$  and  $S$  being the length and area, respectively, of the superlattice, the exciton wave functions have the normalization property  $\langle \Psi_{\vec{K}QNmp} | \Psi_{\vec{K}'Q'N'm'p'} \rangle = \delta_{\vec{K}\vec{K}'} \delta_{QQ'} \delta_{NN'} \delta_{mm'} \delta_{pp'}$ . In addition, we note that the longitudinal size of the exciton state should be much smaller than the magnetic length,  $\bar{z} \ll a_B$ , in order to justify the employed above adiabatic separation of the fast in-plane and slow longitudinal internal motions.

### III. EXCITON STATES

To study the dependencies of the exciton absorption spectrum on the SL parameters and the external fields we consider below the cases amenable to analytical approximations for the binding potential (18). To simplify the derivations, we adopt  $\vec{K} = K\vec{e}_x$  for the exciton in-plane momentum and  $\vec{F} = F\vec{e}_y$  for the external electric field, which yields  $\rho_0 = (\hbar/eB)[K - (M/\hbar B)F]$ . Below we distinguish two cases,  $\rho_0 \ll a_B \ll a_0$  and  $a_B \ll \rho_0 \ll a_0$ .

**A. The case  $\rho_0 \ll a_B \ll a_0$**

Let us first derive an asymptotic expression for the potential for  $\rho_0 \simeq 0$ , when the values of the in-plane exciton momentum  $K$  and electric field  $F$  do not effect the relative longitudinal motion. Since the optically active exciton transitions are proportional to  $|\Psi(\vec{r}_e = \vec{r}_h)|^2$  [27], we have to set the magnetic quantum number  $m = 0$ . The potential  $\bar{U}_N = \bar{U}_{N0}$  acquires the form of the triangular quantum well,

$$\bar{U}_N(z; 0) = \bar{U}_N(0; 0) + eF_0|z|, \quad (21)$$

where

$$\begin{aligned} \bar{U}_N(0; 0) &= \frac{e^2 \beta_N}{4\pi \varepsilon_0 \varepsilon a_B}, \quad F_0 = \frac{e}{4\pi \varepsilon_0 \varepsilon a_B^2}, \\ \beta_N &= -\sqrt{\frac{\pi}{2}} \sum_{j=0}^N \frac{[(2j-1)!!]^2 [2(N-j)-1]!!}{2^{N+j} (N-j)! (j!)^2}. \end{aligned} \quad (22)$$

With increasing  $\rho_0$  the potential well becomes more shallow. For  $\rho_0 \ll a_B$  we obtain for the ground  $N = 0$  Landau states

$$\bar{U}_0(z; \rho_0) = \left(1 - \frac{s}{2}\right) \bar{U}_0(0; 0) + (1-s)eF_0|z|, \quad (23)$$

where  $s = \rho_0^2/(2a_B^2) \ll 1$ . When  $s$  approaches unity ( $\rho_0 = \sqrt{2}a_B$ ), the potential becomes

$$\bar{U}_0(z; \rho_0) = A\bar{U}_0(0; 0) + \exp(-1)eF_0|z|, \quad (24)$$

where

$$A \simeq 2\pi^{-3/2} \int_0^\infty \frac{x e^{-x^2}}{1+x} \left( -\ln[(x-1)^2] + \ln x + 2 \ln \left[ 8 \left( 1 + \sqrt{2} \right) \right] \right) dx \simeq 0.80. \quad (25)$$

The solution for the ground  $p = 1$  state in a one-dimensional triangular quantum well (21) was originally obtained by Kohn and Luttinger [23]. In general, a routine mathematics yields the orthonormalized optically active even-parity wave functions  $\psi_p(z)$  for the ground and excited  $p = 1, 2, 3, \dots$  states in terms of the Airy functions  $\text{Ai}(\xi)$  [28]. For the potential (21) we obtain

$$\begin{aligned} \psi_p(z) &= D_1(p) \text{Ai} \left( \frac{|z| - z_0}{z_1} \right), \quad D_1(p) = [-2c_p z_1 \text{Ai}^2(c_p)]^{-1/2}, \\ z_0 &= \frac{W_{Np} - \bar{U}_N(0; 0)}{eF_0}, \quad z_1 = \left[ \frac{\mu a_0 a_B^2}{2m_\parallel(Q)} \right]^{1/3}, \end{aligned} \quad (26)$$



where

$$W_{Np} = \bar{U}_N(0;0) - \frac{\hbar e B}{\mu} \left[ \frac{\mu a_B^2}{2m_{\parallel}(Q)a_0^2} \right]^{1/3} c_p \quad (27)$$

are the corresponding eigenenergies, see Eq. (16). The coefficients  $c_p$  are the roots of the equation  $\text{Ai}'(c_p) = 0$  which yields  $c_1 = -1.02$ ,  $c_2 = -3.25$ ,  $c_3 = -4.82$ ,  $\dots$ , and  $\text{Ai}(c_1) = 0.54$ ,  $\text{Ai}(c_2) = -0.42$ ,  $\text{Ai}(c_3) = 0.38$ ,  $\dots$ . For the potentials (23) and (24), the analytical results for the wave functions and the energies are transformed accordingly:  $\bar{U}_N(0;0)$  and  $F_0$  are replaced by  $(1 - 0.5s)\bar{U}_0(0;0)$  and  $(1 - s)F_0$ , respectively, for the potential (23), and by  $A\bar{U}_0(0;0)$  and  $\exp(-1)F_0$ , respectively, for the potential (24). The inter-level distances  $\Delta W_{Np} = W_{N,p+1} - W_{Np}$  become smaller in energy.

The parameter  $z_1$  quantifying the extension of the exciton wave function (26) along the magnetic field should respect the applied above continual and adiabatic approximations. Therefore, the analytical approximations (26) and (27) for the exciton quantum states require fulfillment of the condition

$$d \ll z_1 \ll a_B \ll a_0. \quad (28)$$

### B. The case $a_B \ll \rho_0 \ll a_0$

In this case the shift  $\rho_0$  in the denominator of the integrand in the potential (18) can be considered large compared to  $\rho$  and  $|z|$ , and the potential can be approximated by

$$\begin{aligned} \bar{U}_{Nm}(z; \rho_0) &= \bar{U}_{Nm}(0; \rho_0) + \frac{1}{2} m_{\parallel}(Q) \Omega^2 z^2, \\ \bar{U}_{Nm}(0; \rho_0) &= -\frac{e^2}{4\pi\epsilon_0\epsilon\rho_0}, \quad \Omega = \left[ \frac{e^2}{4\pi\epsilon_0\epsilon m_{\parallel}(Q)\rho_0^3} \right]^{1/2}. \end{aligned} \quad (29)$$

The optically active even-parity orthonormalized wave functions  $\psi_p(z)$ ,  $p = 0, 2, 4, \dots$  are the harmonic-oscillator functions

$$\begin{aligned} \psi_p(z) &= D_2(p) \exp(-\xi^2/2) H_p(\xi), \\ D_2(p) &= (z_2 \sqrt{\pi} p! 2^p)^{-1/2}, \quad \xi = \frac{z}{z_2}, \quad z_2 = \left( \frac{\hbar}{m_{\parallel}(Q)\Omega} \right)^{1/2}, \end{aligned} \quad (30)$$

where  $H_p(\xi)$  are the Hermite polynomials [28]. The corresponding eigen energies are

$$W_{Nmp} = \bar{U}_{Nm}(0; \rho_0) + \hbar\Omega \left( p + \frac{1}{2} \right). \quad (31)$$

The analytical results (30) and (31) require the fulfillment of the condition

$$d \ll z_2 \ll a_B \ll \rho_0 \ll a_0, \quad (32)$$

which justifies both the adiabatic and continual approximations employed.

#### IV. SPECTRUM OF THE EXCITON ABSORPTION. RESULTS AND DISCUSSION

The exciton optical absorption coefficient can be calculated as follows [29]

$$\alpha = \frac{n_0 \hbar \omega \Pi}{c \tilde{U} S N d}, \quad (33)$$

where  $n_0$  is the refractive index,  $c$  is the speed of light,  $\tilde{U} = \varepsilon_0 n_0^2 \mathcal{E}_0^2$  is the energy density of the optical radiation electric field  $\vec{\mathcal{E}} = \vec{\eta} \mathcal{E}_0 \exp(-i\omega t)$  with  $\vec{\eta}$  being a unit polarization vector, and

$$\Pi = \frac{1}{t} \sum \left| \frac{1}{i\hbar} \int_0^t d\tau \langle \Psi | \mathcal{P}_{eh}(\tau) | \Psi_0 \rangle \exp \left( \frac{i}{\hbar} E \tau \right) \right|^2 \quad (34)$$

is the transition rate. The summation in Eq. (34) is performed over the exciton states with the wave functions  $\Psi = \Psi_{\vec{K}QNmp}(\vec{r}_e, \vec{r}_h)$  and the energies  $E = E_{\vec{K}QNmp}$ ,  $\Psi_0 = \delta(\vec{r}_e - \vec{r}_h)$  [27]. The matrix element  $\langle \Psi | \mathcal{P}_{eh}(\tau) | \Psi_0 \rangle$  involving integration over  $\vec{r}_e$  and  $\vec{r}_h$  is determined by the operator of electric dipole transitions [30]

$$\mathcal{P}_{eh}(t) = \frac{2i\hbar e \mathcal{E}_0}{m_0 E_g} |\vec{\eta} \vec{p}_{eh}| \delta_{\vec{q}, \vec{P}} \cos(\omega t), \quad (35)$$

where  $E_g \simeq \hbar\omega$ ,  $m_0$  is the mass of the free electron,  $\vec{p}_{eh}$  is a momentum averaged with the Bloch amplitudes of the electron and hole bands, and  $\vec{P}$  and  $\vec{q}$  are the exciton and photon wave vectors, respectively.

Using the exciton wave functions derived in the previous section, we obtain a spectral form of the absorption coefficient,

$$\alpha = \alpha^{(0)} \sum_{Nmp} f_{Nmp} \delta(E_{Nmp} - \hbar\omega), \quad \alpha^{(0)} = \frac{\pi \hbar e^2}{\varepsilon_0 n_0 m_0 c S L}, \quad (36)$$

where

$$f_{Nmp} = \frac{2|\vec{\eta}\vec{p}_{eh}|^2}{m_0\hbar\omega a_0^3} G_{Nmp} \quad \text{and} \quad G_{Nmp} = a_0^3 |\Lambda_{Nm}(\rho_0)\psi_p(0)|^2 \quad (37)$$

are the oscillator strength density and the dimensionless oscillator strength, respectively. The energies  $E_{Nmp}$  are determined by Eq. (13) for conserved total momentum,  $\vec{q} = \vec{P}$ , as implied by the factor  $\delta_{\vec{q},\vec{P}}$  in Eq. (35).

Analytical estimates, useful for the analysis of the exciton absorption, can be obtained for the two distinct regimes considered in the previous section. For each regime we will discuss the dependencies on the electric  $F$  and magnetic  $B$  field strengths for the binding energies  $E_{Nmp}^{(b)} = |W_{Nmp}|$ , for the positions  $E_{Nmp}$  of spectral lines in the exciton absorption, and for the oscillator strengths  $G_{Nmp}$ . We will also analyze the dependencies of these quantities on the angle  $\vartheta$  which determines the direction of the photon wave-vector  $\vec{q} = K\vec{e}_x + Q\vec{e}_z$ , where  $K = q \sin \vartheta$  and  $Q = q \cos \vartheta$ , in the  $x - z$  plane.

#### A. The case $\rho_0 \ll a_B \ll a_0$

In the case of small  $\rho_0$  values we may assume  $K \simeq 0$ ,  $F \simeq 0$  and estimate the oscillator strength as

$$G_{N0p} = \frac{1}{2\pi} \left( \frac{a_0}{a_B} \right)^2 \frac{1}{(-2c_p)} \left[ \frac{2m_{\parallel}(Q)}{\mu} \left( \frac{a_0}{a_B} \right)^2 \right]^{1/3}, \quad p = 1, 2, 3, \dots, \quad (38)$$

where the coefficients  $c_p$  are the same as in Eq. (27). The spectral peak positions  $E_{N0p}$  can be calculated from Eqs. (13) and (27) for  $m = 0$  and  $\vec{K} = \vec{\tilde{K}} = 0$ .

The account for small values of the in-plane exciton momentum and the electric field has a minor effect on the exciton binding energies and the absorption spectrum. Notice that the first term in Eq. (27) significantly exceeds the second term, as it is reflected by the condition  $z_1 \ll a_B$  required for the adiabatic approximation. It follows from Eq. (27) that, for a given Landau level number  $N$ , both the binding energies  $E_{Np}^{(b)} = E_{N0p}^{(b)}$  and the energy gaps  $\Delta E_{Np}^{(b)} = E_{Np}^{(b)} - E_{N,p+1}^{(b)}$  between the neighboring levels increase with increasing magnetic field strength  $B$  and decrease with increasing quantum number  $p$ . It also follows that the energies  $E_{Np}^{(b)}$  grow with the value  $Q$  of the exciton longitudinal momentum. The binding properties are demonstrated in Fig. 1 for the ground-state binding energy  $E_{001}^{(b)}$  calculated as a function of  $B$  and  $Q$  according to Eq. (27).

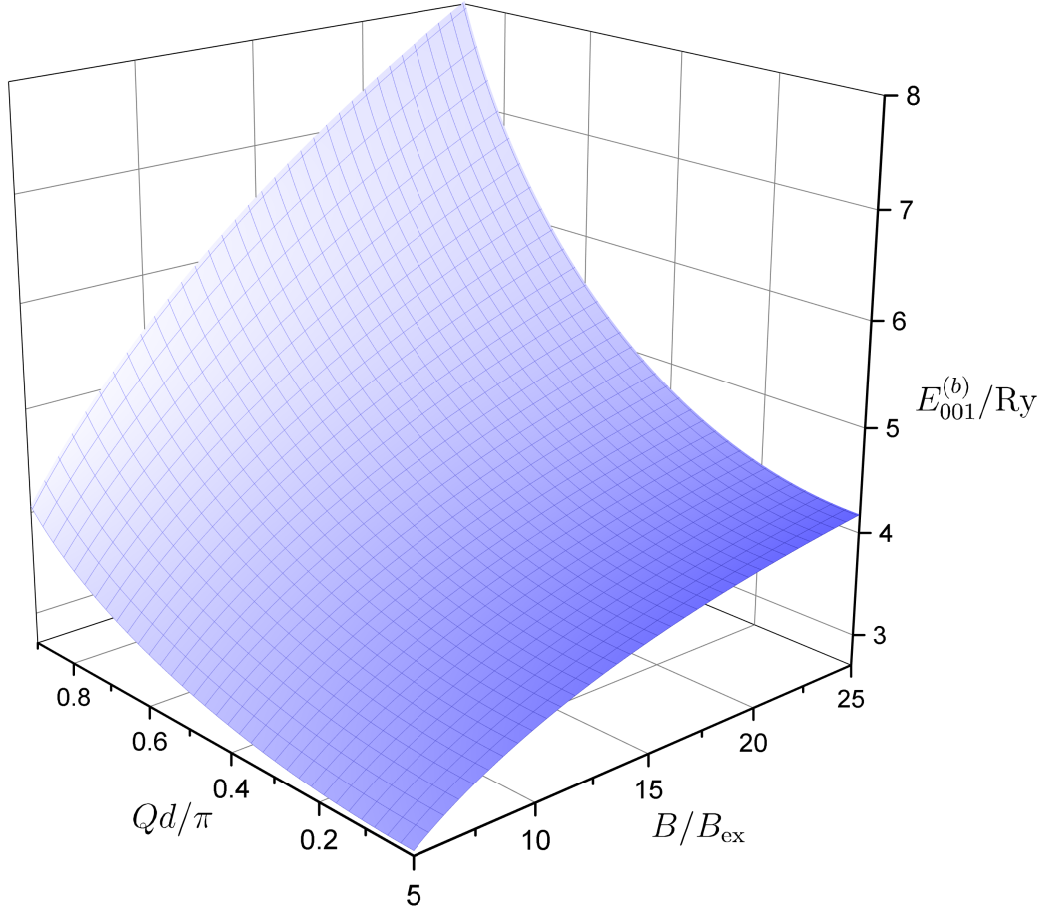


FIG. 1. The exciton ground state binding energy according to Eq. (27) for  $\mu/m_{\parallel}(0) = 0.22$ . The energy (in units of the exciton Rydberg constant) is shown as a function of the magnetic field strength (in units of  $B_{\text{ex}} = \hbar/(ea_0^2)$ ) and the longitudinal component of the exciton wave vector (in units of  $\pi/d$ ).

With increasing  $N$  the coefficient  $\beta_N$  in Eq. (21) decreases providing smaller values  $|\bar{U}_N(0,0)|$  for the depth of the triangular potential well. As a result, the  $N$ -series of the exciton levels move to the region of smaller energies for larger  $N$ .

Overall, the absorption spectrum (36) comprises a sequence of series of peaks corresponding to varying  $p$  for different numbers  $N$ . The peak positions in each series are adjacent from the lower energies to the thresholds

$$\hbar\omega_N = \mathcal{E}_g + T(Q) + \frac{\hbar e B}{2\mu} (2N + 1), \quad (39)$$

with the distance  $\hbar e B/\mu$  between the neighboring thresholds considerably exceeding the energy domain  $\approx |\bar{U}_N(0,0)|$  of the series. With increasing magnetic field strength  $B$  and the

longitudinal momentum  $Q$  the  $Np$  peaks shift toward higher frequencies, while the distances between the neighboring  $Np$  and  $N, p + 1$  peaks increase with increasing magnetic field strength and decrease with increasing longitudinal momentum. For given  $N$ , the neighboring peaks come closer to each other with increasing  $p$ , i.e. with the peak positions approaching the thresholds (39). The peak intensities  $f_{Np}$  increase as  $\sim B^{4/3}$  with the magnetic field strength, and they decrease with growing quantum number  $p$ . All the  $N$ -series of peaks are equal in intensity. Notice that, analogously to the binding energies, the peak intensities increase as the longitudinal momentum value  $Q$  approaches the Brillouin zone boundary. The above-discussed properties are illustrated in Fig. 2 by the intensity  $G_{001}$  of the ground-state exciton absorption calculated according to Eq. (38) as a function of the magnetic field  $B$  and the longitudinal momentum  $Q$  for  $\mu/m_{\parallel}(0) = 0.22$ .

### B. The case $a_B \ll \rho_0 \ll a_0$

In contrast to the previous case, the quantity  $\rho_0$  is now not close to zero, and the in-plane total wave vector  $K$  and the electric field  $F$  significantly influence the exciton binding energies and the absorption spectrum. The oscillator strengths become

$$G_{Nmp} = \frac{1}{2\pi} \left( \frac{a_0}{a_B} \right)^2 \frac{s^{2N+|m|}}{N!(N+|m|)!} \exp(-s) \left[ \frac{m_{\parallel}(Q)}{\mu} \left( \frac{a_0}{\rho_0} \right)^3 \right]^{1/4} \frac{[(p-1)!!]^2}{\sqrt{\pi} p!}, \quad (40)$$

where  $s = \rho_0^2/(2a_B^2) \gg 1$ ,  $N, |m| = 0, 1, 2, \dots$ ,  $p = 0, 2, 4, \dots$ . The peak positions  $E_{Nmp}$  are determined by Eqs. (13) and (31). To simplify the analysis of the effects of the electric field and exciton momentum, we will consider the cases where  $\rho_0$  is dominantly determined by either  $F$  or  $K$  values.

#### B1. The case $a_B \ll \rho_0 \ll a_0$ , $K \ll MF/(\hbar B)$

In this case the electric field influences the exciton absorption to a much stronger extent than the in-plane momentum. Because of the condition  $z_2 \ll a_B$  required by the adiabatic approximation, the binding potential (29) and the quantum energies (31) are dominated by the first terms of the corresponding expressions. It follows then that, both the binding energies  $E_p^{(b)} = |W_{Nmp}^{(b)}|$  and the distances  $\Delta E^{(b)} = E_p^{(b)} - E_{p+2}^{(b)} = 2\hbar\Omega$  between the neighboring levels decrease with increasing the strength of the electric field. Increasing the

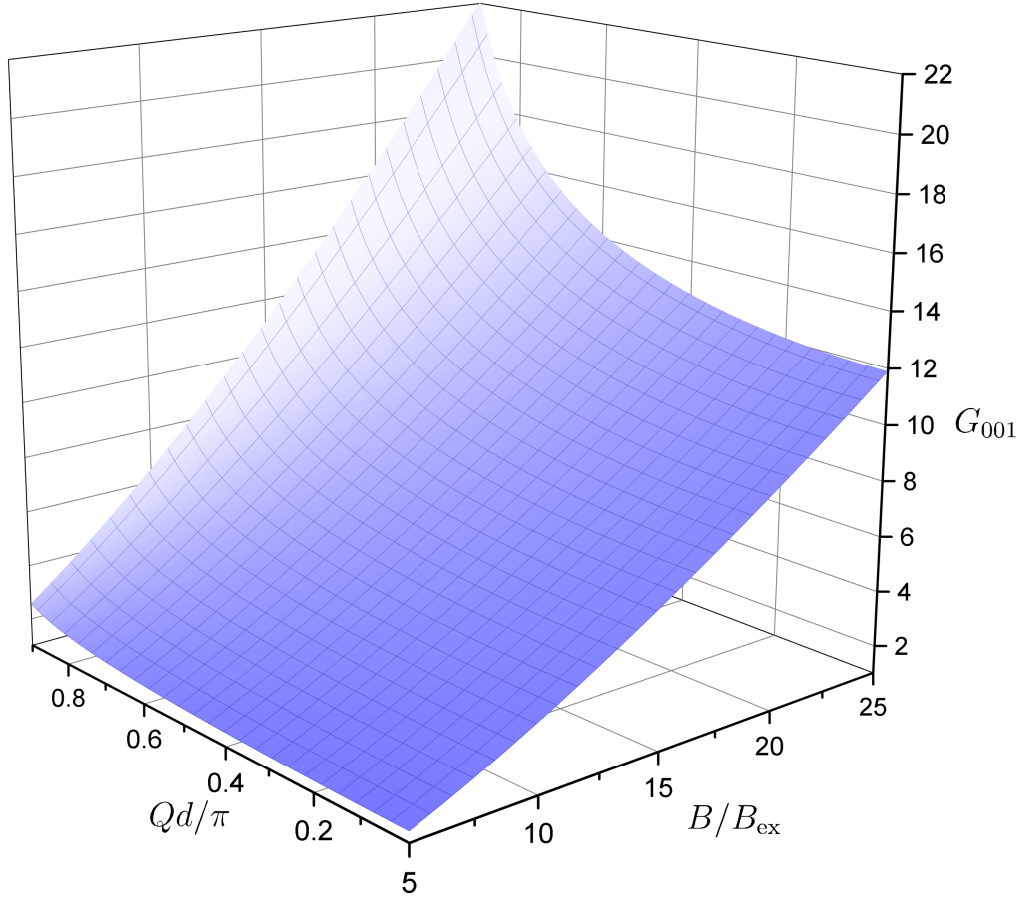


FIG. 2. The dependency of the dimensionless oscillator strength  $G_{001}$  for the ground peak in the exciton absorption on the magnetic field strength  $B$  and the longitudinal exciton wave vector  $Q$ . Units for  $B$  and  $Q$  as in figure 1.

longitudinal momentum  $Q$  increases the binding energies  $E_p^{(b)}$  and decreases the gaps  $\Delta E^{(b)}$ . As in the previous case, the binding energies and the gaps are larger for a stronger magnetic field. They scale with the field strength as  $E_p^{(b)} \sim B^2$  and  $\Delta E^{(b)} \sim B^3$ . Notice that in the regime considered the binding energies do not depend on the quantum numbers  $N$  and  $m$ . In Fig. 3, we show the ground-state ( $p = 0$ ) binding energies (Eq. (31)) as functions of the electric  $F$  and magnetic  $B$  field strengths for  $\mu/m_{\parallel}(0) = 0.22$ ,  $\mu/M = 0.12$ . Fig. 4 shows the dependence on  $F$  and  $B$  for the energy separation  $\Delta E^{(b)}$  between the equidistant exciton levels in each series.

The lines in the exciton absorption spectrum (36) arise at the frequencies corresponding to the different sets  $Nmp$  of the quantum numbers and group for each pair  $Nm$  in the series.

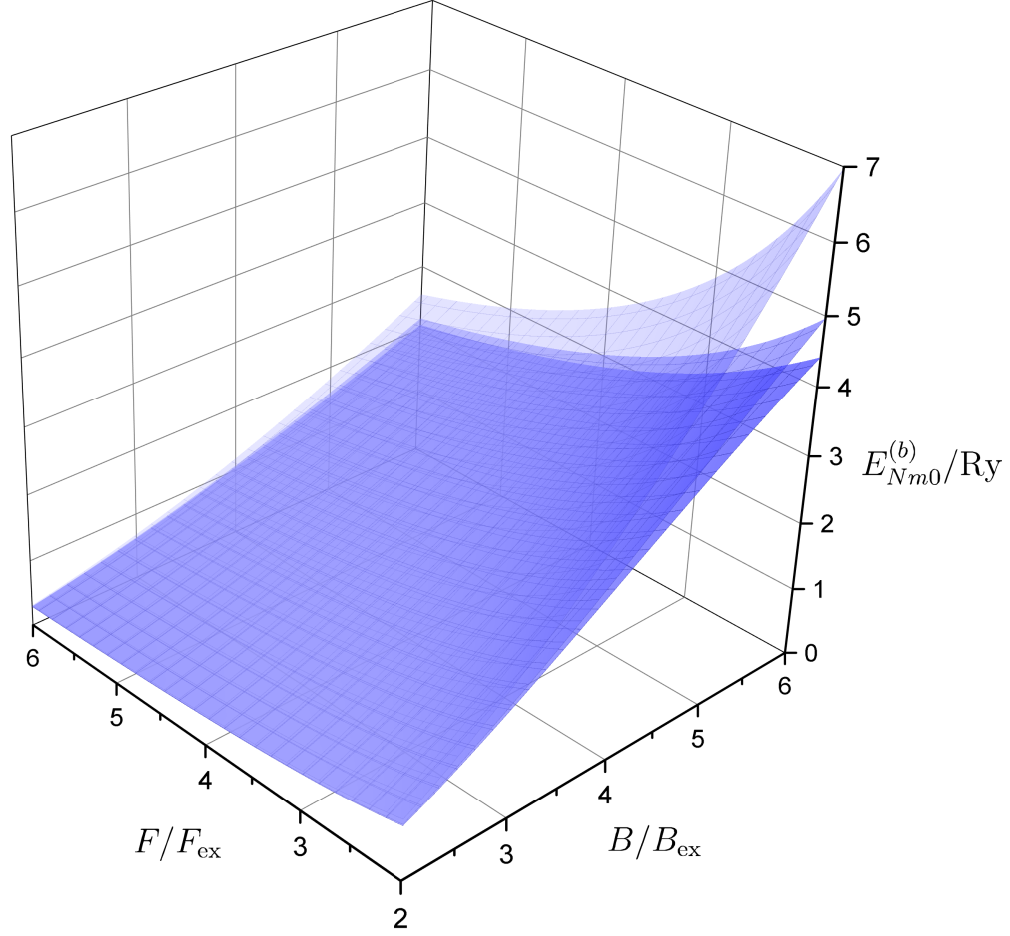


FIG. 3. The binding energies (in units of the exciton Rydberg constant) of the exciton  $p = 0$  states. The energies are the same for all  $N, m$  series of states and calculated according to Eq. (31) for  $\mu/m_{\parallel}(0) = 0.22$  and  $\mu/M = 0.12$ . The surface plots show the energies as functions of the strengths of the external electric  $F$  and magnetic  $B$  fields (scaled with  $F_{\text{ex}} = \text{Ry}/(ea_0)$  and  $B_{\text{ex}} = \hbar/(ea_0^2)$ , respectively), for three different values of the longitudinal wave vector:  $Qd/\pi = 0$  (bottom surface),  $Qd/\pi = 0.45$  (middle surface), and  $Qd/\pi = 0.9$  (upper surface).

Notice that the line series  $m \neq 0$  result from the presence of an in-plane electric field. With increasing  $p$  the series saturate, coming from lower frequencies, towards the thresholds

$$\hbar\omega_{Nm} = \mathcal{E}_g + T(Q) + \frac{\hbar e B}{2\mu} \left( 2N + |m| + \delta \cdot m + 1 \right) - \frac{MF^2}{2B^2}, \quad (41)$$

which now depend on the field strengths. The gaps  $\sim \hbar e B/\mu$  between the thresholds significantly exceed the energy ranges  $|\bar{U}_{Nm}(0, \rho_0)|$  of the series of absorption peaks. In each series the peak positions are equidistant and separated by the interval  $\Delta E_{Nmp}^{(b)} = 2\Omega$  which

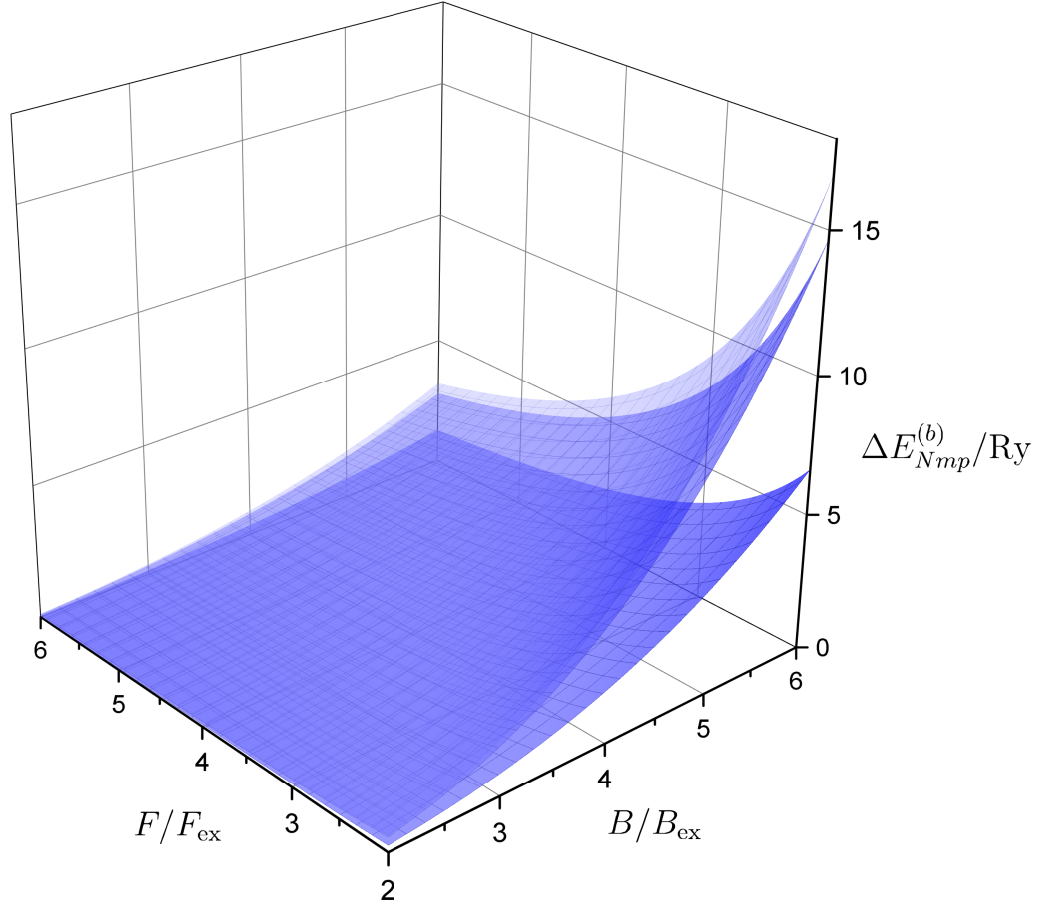


FIG. 4. Surface plots showing the distance between the neighboring exciton absorption peaks (in units of the exciton Rydberg constant) as a function of  $F/F_{\text{ex}}$  and  $B/B_{\text{ex}}$  for the same parameters as in figure 3. The upper, middle and bottom surfaces correspond to the values 0, 0.45 and 0.9 of  $Qd/\pi$ , respectively.

does not depend on  $p$  in the harmonic approximation (31). Increasing the electric field strength shifts the  $Nm$  series to lower frequencies and narrows the series' energy ranges  $|\bar{U}_{N,m}(0, \rho_0)| \sim F^{-1}$ . The inter-peak separations in each series decrease with increasing electric field and exciton longitudinal momentum,  $\Omega \sim (m_{\parallel}(Q)F^3)^{-1/2}$ .

According to Eqs. (37) and (40), the oscillator strengths  $f_{Nmp}$  increase with increasing magnetic field strength  $B$ . Their dependence on the electric field strength  $F$  is non-monotonic for all except the ground ( $N = m = 0$ ) series. For weak electric fields,  $s \ll 1$ , the ground series which is optically active at  $F = 0$  reduces in intensity as  $F$  increases, whereas the series with  $m \neq 0$  become more intense. As  $F$  increases in the range of moderate,  $s \simeq 1$ ,



and large,  $s \gg 1$ , strengths, the oscillator strengths in all series decrease. The maximal intensities in optical absorption increase with the exciton wave number  $Q$  approaching the Brillouin zone boundary. The oscillator strengths decrease with increasing  $p$ . For illustration, we show in Fig. 5 the oscillator strengths  $G_{00p}$  as functions of  $F$  and  $Q$  for the exciton absorption to the ground  $p = 0$  and first excited  $p = 2$  states. They are determined according to Eq. (40) with the choice  $\mu/m_{\parallel}(0) = 0.22$  and  $(a_0/a_B)^2 = 5$ .

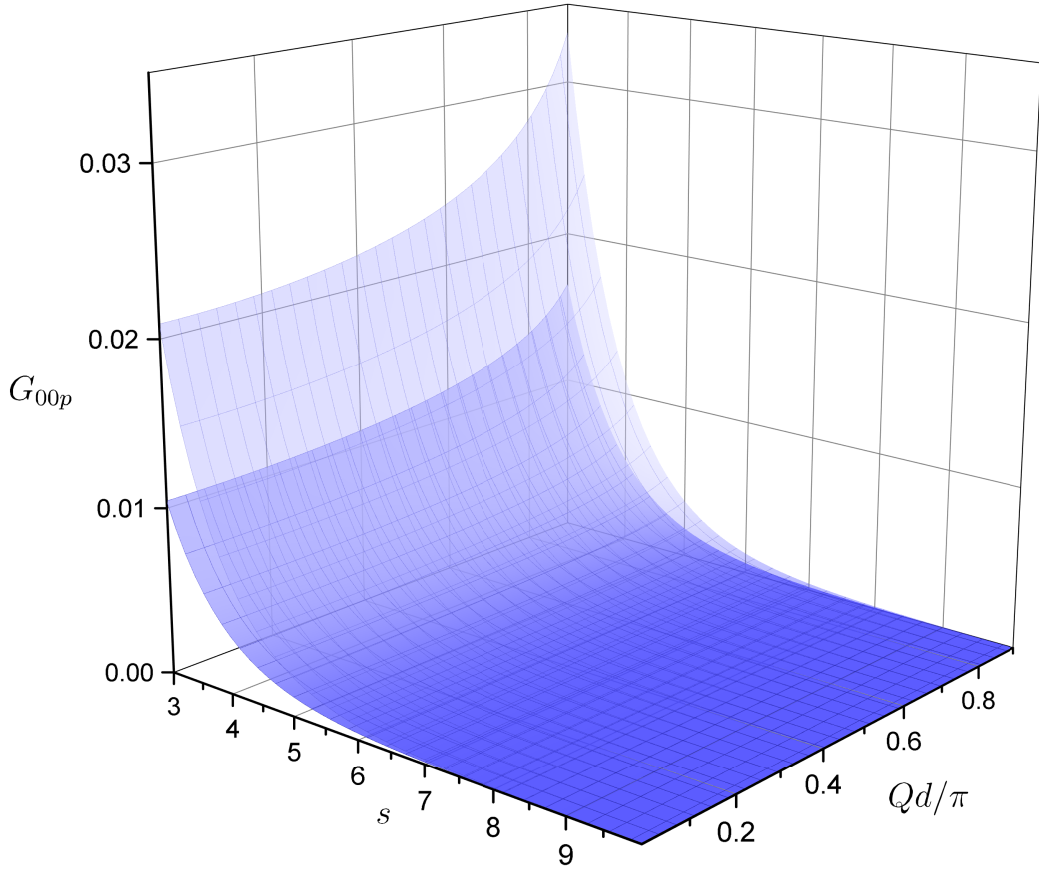


FIG. 5. The dimensionless oscillator strengths  $G_{00p}$  of the transitions to the ground  $N = m = p = 0$  (upper surface) and first excited  $N = m = 0, p = 2$  (bottom surface) exciton states. The oscillator strengths are determined according to Eq. (40) for  $\mu/m_{\parallel}(0) = 0.22$  and  $B/B_{\text{ex}} = 5$  and shown as functions of the electric field strength  $F \sim s^{1/2}$  ( $s = \rho_0^2/(2a_B^2)$ ) and the longitudinal exciton wave vector scaled with the Brillouin zone boundary  $\pi/d$ .

**B2. The case  $a_B \ll \rho_0 \ll a_0$ ,  $K \gg MF/(\hbar B)$**

In this situation the in-plane exciton momentum dominates the electric field effects influences of the exciton absorption. For better transparency of the effect of in-plane exciton motion we put the length of the photon wave vector to be close to the Brillouin zone boundary, and the electron and hole minibands to coincide with each other. The exciton absorption coefficient  $\alpha$ , peak positions  $E_{Nmp}$  and the oscillator strength  $f_{Nmp}$  can then be derived from Eqs. (36), (37), (31), (40) with account for the relations

$$K = q \sin \vartheta, \quad Q = q \cos \vartheta, \quad q = \pi/d, \quad \Delta_e = \Delta_h \equiv \Delta_0, \\ \rho_0 = \frac{\pi a_B^2}{d} \sin \vartheta, \quad \Omega = \frac{\hbar}{a_B^2 \mu} \frac{d}{a_B} \left[ \frac{1}{\pi^3} \frac{\mu}{m_{\parallel}(0)} \frac{d}{a_0} \frac{\cos\left(\frac{\pi}{2} \cos \vartheta\right)}{\sin^3 \vartheta} \right]^{1/2}, \quad (42)$$

where  $\vartheta$  is the angle between the photon wave vector  $\vec{q}$  and the SL axis.

The analysis shows that deviation of the vector  $\vec{q}$  from the SL axis results in decreasing binding energies  $E_{Nmp}^{(b)} = |W_{Nmp}|$  (cf. Eq. (31)) and the energy gaps  $2\hbar\Omega$  between the neighboring  $p$ -states. The peak positions  $E_{Nmp} = E_{Nm} - E_{Nmp}^{(b)}$  shift towards higher energies, though the thresholds

$$E_{Nm} = \mathcal{E}_g + 2\Delta_0 \sin^2\left(\frac{\pi}{4} \cos \vartheta\right) + \frac{\hbar e B}{2\mu} (2N + |m| + \delta m + 1), \quad (43)$$

become lower in energy. The oscillator strengths  $f_{Nmp}$  (see Eqs. (37) and (40)) reduce in magnitude. The numerical results are presented in Figs. 6 and 7. Fig. 6 shows the ground state binding energy  $E_{N=0}^{(b)}$  calculated according to Eq. (31) for  $\mu/m_{\parallel}(0) = 0.22$  and different values  $\nu = a_0 d/a_B^2$ . Fig. 7 shows the oscillator strength  $G_{000}$  of the transition to the ground exciton state  $N = m = p = 0$  calculated according to Eq. (40) for the same  $\mu/m_{\parallel}(0)$  ratio and different pairs of the values  $\zeta = a_0/a_B$  and  $\eta = a_B/d$ . A significant effect of the external electric and magnetic fields and of the SL parameters studied in the figures is related to the condition (32) in which

$$z_2 = a_B \left[ \pi^3 \frac{\mu}{m_{\parallel}(0)} \zeta \eta^3 \cos\left(\frac{\pi}{2} \cos \vartheta\right) \sin^3 \vartheta \right]^{1/4}. \quad (44)$$

In the presence of crossed electric and magnetic fields, the exciton in SL displays an *inversion effect*: changing orientation of any of the three vectors,  $\vec{F}$ ,  $\vec{B}$  and  $\vec{K} = \vec{q}_{\perp}$ , to the opposite ones results in a change of the exciton states and absorption spectrum. Originally

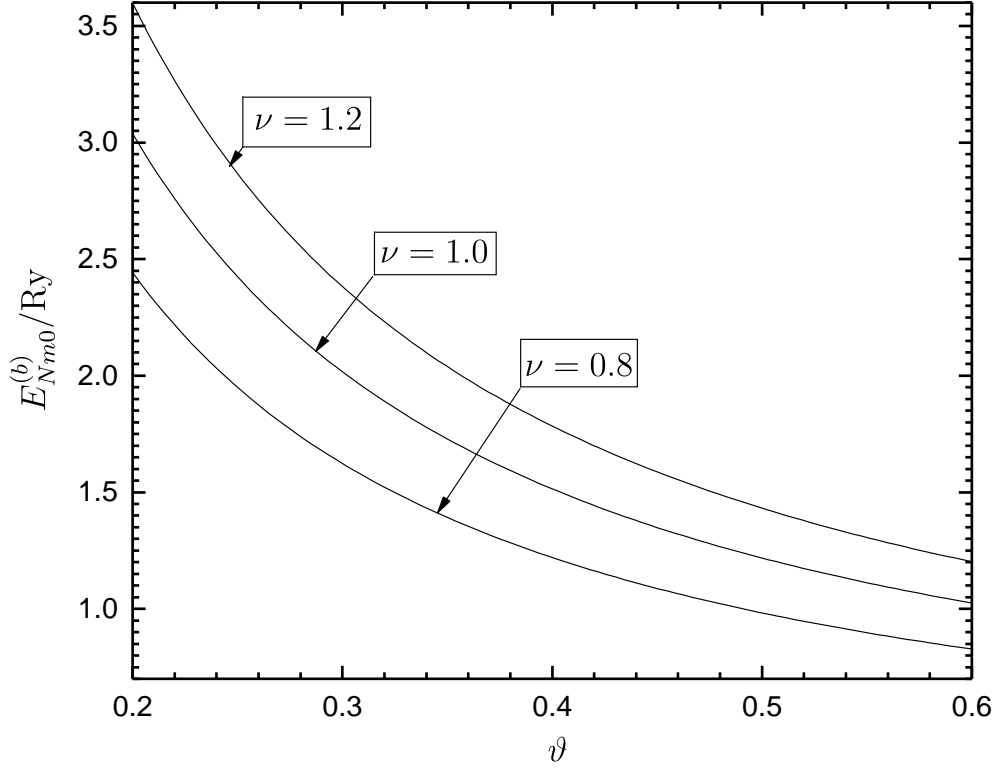


FIG. 6. The dependence of the exciton binding energies  $E_{Nm0}^{(b)}$  (in units of the exciton Rydberg constant) on the angle  $\theta$  between the photon wave vector and the SL axis. The binding energies are the same for all  $N$  and  $m$  and determined according to Eq. (31). The results correspond to  $\mu/m_{\parallel}(0) = 0.22$  and three different values for  $\nu = a_0 d/a_B^2$  (indicated near the curves).

this phenomenon has been studied in connection with the Stark effect in the presence of magnetic fields in the CdS bulk material [31]. According to the analytical results presented here, the dependence of the peak positions  $\hbar\omega = E_{Nmp}$  on the orientation of the vectors  $\vec{F}$ ,  $\vec{B}$  and  $\vec{K}$  follows from Eqs. (13) and (31). A particularly important prediction of our analysis is the existence of a critical electric field  $F_{\text{cr}} = \hbar BK/M$  for which  $\rho_0 = 0$  and the distances between the neighboring  $p$  and  $p+1$  spectral peaks reach a maximum determined by Eq. (27). This implies that by varying the strength of the electric field  $F$  in an experiment and measuring the maximum distance  $\Delta\omega$  between the ground  $p=1$  and first excited  $p=2$

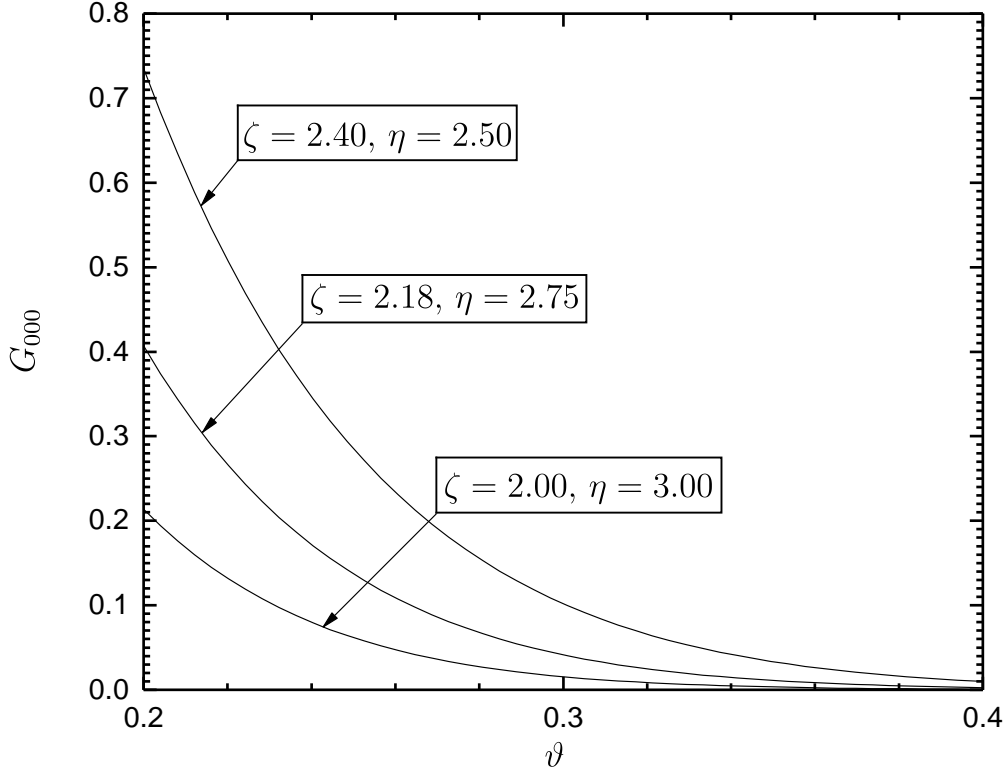


FIG. 7. The dimensionless oscillator strength  $G_{000}$  for the ground peak of the exciton absorption as a function of the angle  $\vartheta$  between the photon wave vector and the SL axis. The oscillator strength is determined according to Eq. (40) for  $\mu/m_{\parallel}(0) = 0.22$  and different pairs of the parameters  $\zeta$  and  $\eta$  as indicated.

exciton peaks one can determine the effective mass  $m_{\parallel}(Q)$  satisfying the equation

$$\Delta\omega = \frac{eB}{\mu} \left( \frac{\mu}{2m_{\parallel}(Q)} \frac{a_B^2}{a_0^2} \right) (c_1 - c_2). \quad (45)$$

In this way it is possible to trace experimentally the dependence on the longitudinal exciton momentum  $Q$  and establish the dispersion law for the exciton in the SL. The latter parameter which is difficult to determine theoretically affects strongly the electronic, optical and transport SL properties.

As originally pointed out in Ref. [22], the applicability of the analytical approach employed here is restricted to the conditions (28) and (32) which involve the SL parameters  $\Delta_{e,h}$ ,  $d$ ,  $\mu$  and the magnetic field strength  $B$ . In order to meet these restrictions for SL which

can be experimentally probed, we consider the GaAs/Al<sub>x</sub>Ga<sub>1-x</sub>As SL for  $x = 0.3$  with period  $d = 2$  nm in a magnetic field  $B = 20$  T. This SL has the following parameters [32]:  $\mathcal{E}_g = 1.52$  eV,  $\mu = 0.06m_0$ ,  $M = 0.5m_0$ , and  $\text{Ry} = 4.7$  meV. Notice that for the chosen SL the conditions (28) and (32) imply the longitudinal effective mass to significantly exceed the reduced mass,  $m_{\parallel}(Q) \gg \mu$ , as well as the minibands  $\Delta_{e,h}$  to be narrow and the period  $d$  to be short. On the other hand, the minibands become wider with decreasing  $\mu$  and  $d$ ,  $\Delta_{e,h} \sim \mu^{-1}d^{-2}$ . This conflict can be softened by fabrication of a SL with an optimal relation between the barrier and well widths [22]. For our analytical estimates we adopt the ratio  $\mu/m_{\parallel}(0) = 0.22$  as the SL parameter, and consider three regimes corresponding to the cases A, B1 and B2, respectively.

### 1. $\rho_0 \ll a_B$

We may set  $F = K = Q = 0$  neglecting thereby the effects of the electric field and exciton momentum on the exciton states and absorption. Then the value of the ground state binding energy estimated according to Eq. (27) is  $E_{001}^{(b)} = |W_{01}| = 11.9$  meV. Notice that in the absence of a magnetic field bound exciton states do not exist [23]. The corresponding dimensionless oscillator strength given by Eq. (38) is  $G_{001} = 1.0$ , and the energy separation between the neighboring Landau series is  $\Delta_L = \hbar eB/\mu = 38.3$  meV.

### 2. $\rho_0 \gg a_B$ , $K = Q = 0$ , $F \neq 0$

As in the previous case, we assume the exciton momentum to be zero. However, the electric field now does not vanish, and we pick a value  $F = 9.0$  kV/cm satisfying the conditions above. The ground exciton state binding energy determined according to Eq. (31) is  $E_{Nm0}^{(b)} = |W_{Nm0}| = 11.3$  meV. Eq. (13) allows to estimate a threshold red shift due to the applied electric field,  $\Delta_F = MF^2/(2B^2) = 2.9$  meV, whereas Eq. (40) yields  $G_{000} = 0.25$  for the dimensionless oscillator strength of the transition to the ground exciton state.

### 3. $\rho_0 \gg a_B$ , $F = 0$ , $K \neq 0$

In order to address the interplay between the longitudinal  $Q = q \cos \vartheta$  and the transverse  $K = q \sin \vartheta$  components of the exciton wave vector we set  $F = 0$  and  $q = \pi/d$ . The results acquire a most simple form for the equal electron and hole miniband widths  $\Delta_e = \Delta_h$ . As already pointed out, the conditions (32) hold for a narrow domain of the angles  $\vartheta$ . Nevertheless, variations of the ground state binding energies and oscillator strengths with  $\vartheta$  can be well distinguished in an experiment. The estimates according to Eqs. (31) and (40) yield  $E_{Nm0}^{(b)} = 10.01 \text{ meV}$ ,  $G_{000} = 0.37$  and  $E_{Nm0}^{(b)} = 13.42 \text{ meV}$ ,  $G_{000} = 1.05$  for the angles  $\vartheta = 0.20$  and  $\vartheta = 0.15$ , respectively.

We believe that our analytical results are in line with the current technological progress in fabricating SLs with a narrow miniband and a short period. The corresponding numerical estimates demonstrate that the fine structure of the exciton magnetoelectroabsorption can be experimentally detected.

## V. CONCLUSIONS

We have studied the quantum states and optical absorption for an exciton in a semiconductor SL subject to external crossed electric and magnetic fields directed perpendicular and parallel to the SL axis, respectively. Analytical results have been obtained for the exciton wave functions and energies as well as for the transition energies and oscillator strengths of the absorption spectra. We have considered the case where the magnetic length considerably exceeds the SL period but is much smaller than the exciton Bohr radius. Here, an adiabatic separation is possible for the two types of internal exciton motions: the fast in-plane motion and the slow longitudinal motion governed by the external magnetic and electric and the internal Coulomb fields, respectively.

We have focused on the fine structure of the exciton energies related to the bound electron-hole states in effective one-dimensional potentials which are triangular-type and oscillator-type for a weak and a strong effective electric field, respectively. The latter field is a combination of the external electric field and a field induced by the exciton center-of-mass motion in the external magnetic field. It was shown that an increase of the magnetic field leads to an increase of the binding energies, of the energy separations between the states, and of

the oscillator strengths of optical transitions. In the opposite positive case, with increasing effective electric field the latter energy and spectral quantities decrease. An inversion effect for the exciton absorption with changing external electric and magnetic fields and switching the directions of the in-plane exciton momentum, has been highlighted. A novel interplay of external crossed fields, transverse and especially longitudinal centre-of-mass and internal exciton motions has been found to occur. The analytical results and numerical estimates obtained can be useful for extending our knowledge on the excitonic magneto-electro-states relevant to micro- and opto-electronics.

- 
- [1] L. Esaki and R. Tsu, IBM J. Res. Dev. **14**, 61 (1970)
  - [2] G. H. Wannier, Phys. Rev. **117**, 432 (1960).
  - [3] L. D. Landau, Zs.f.Phys. **64**, 629 (1930)
  - [4] J. Bleuse, G. Bastard and P. Voisin, Phys. Rev. Lett. **60**, 220 (1988)
  - [5] M. M. Dignam and J. E. Sipe, Phys. Rev. Lett. **64**, 1797 (1990)
  - [6] E. E. Mendez, F. Agullo-Roeda and J. M. Hong, Phys. Rev. Lett. **60**, 2426 (1988)
  - [7] F. Agullo-Roeda J. A. Brum, E. E. Mendez and J. M. Hong, Phys. Rev. B, **41**, 1676 (1990)
  - [8] J. C. Maan, Surf. Sci. **196**, 518 (1988)
  - [9] J. C. Maan, Y. Guldner, J. P. Vieren, P. Voisin, M. Voos, L. L. chang and L. Esaki, Solid State Commun. **39**, 683 (1981)
  - [10] M. Pacheco, Z. Barticevic, F. Claro, Phys. Rev. B, **46**, 15200 (1992)
  - [11] A. M. Berezhtkovskii and R. A. Suris, Sov. Phys. JETP, **59**, 109 (1984)
  - [12] A. M. Berezhtkovskii and R. A. Suris, Sov. Phys. Semicond, **18**, 764 (1984)
  - [13] B. S. Shchamkhalova and R. A. Suris, Superlatt. and Microstruct., **17**, 147 (1995)
  - [14] J. N. Zuleta and E. Reyes-Gomes, Physica B **488**, 72 (2016)
  - [15] D. F. Nelson, R. C. Miller, C. W. Tu and S. K. Sputz, Phys. Rev. B, **36**, 8063 (1987)
  - [16] A. Chomette, B. Lambert, B. Deveaud, F. Clerot, A. Regreny and G. Bastard, Europhys. Lett. **4**, 461 (1987)
  - [17] M. Pacheco, Z. Barticevic and F. Claro, J. Phys.: Condens. Matter, **5**, A363 (1993)
  - [18] M. M. Dignam and J. E. Sipe, Phys. Rev. B, **45**, 6819 (1992)
  - [19] G. Bastard, *Wave mechanics applied to semiconductor heterostructures*, Les editors de

- Physique, Paris (1990)
- [20] *Low-dimensional semiconductor structures*, ed. by K. Barnham and D. Vvedensky, Cambridge University Press (2001)
  - [21] S. Glutsch, *Excitons in low-Dimensional Semiconductors: Theory, Numerical Methods, and Applications*, Springer Series in *Solid State Sciences* 141, Berlin and Heidelberg (2004)
  - [22] R. A. Suris, *Semiconductors*, **49**, 807 (2015)
  - [23] W. Kohn, J. M. Luttinger, *Phys. Rev.* **98**, 915 (1955)
  - [24] B. S. Monozon and P. Schmelcher, *Physica B* **507**, 61 (2017)
  - [25] L. P. Gor'kov and I. E. Dzyaloshinskii, *Sov. Phys. JETP* **26**, 449 (1967)
  - [26] I. S. Gradshteyn and I. M. Ryzhik, *Tables of Integrals, Series and Products*, Academic, New York, 1980
  - [27] R. J. Elliot, *Phys. Rev.* **108**, 1384 (1957).
  - [28] *Handbook of Mathematical Functions*, edited by M. Abramowitz and I. A. Stegun (Dover, New York, 1972)
  - [29] B. S. Monozon and A. G. Zhilich, *Phys. Solid. State*, **37**, 508 (1995)
  - [30] M. H. Weiler, M. Reine, B. Lax, *Phys. Rev.* **171**, 949 (1968).
  - [31] D. G. Thomas, J. J. Hopfield, *Phys. Rev. Lett.* **5**, 505 (1960); *Phys. Rev.* **124**, 657 (1961)
  - [32] P. Harrison, *Quantum Wells, Wires and Dots* (Wiley, New York, 2000), p. 183